Transport phenomena in the SOL of ASDEX Upgrade

Schrittwieser, R.; Mehlmann, F.; Ionita, C.; Naulin, Volker; Rasmussen, Jens Juul; Müller, H.W.; Vianello, N.; Maszl, Ch.; Rohde, V.; Zuin, M.; Cavazzana, R.; Maraschek, M.

Publication date:
2010

3rd EFDA Transport Topical Group Meeting, combined with the 15th EU-US Transport Task Force Workshop, Córdoba, Spain, September 7 – 10, 2010

Transport phenomena in the SOL of ASDEX Upgrade

R. Schrittwieser[1], F. Mehlmann[1], C. Ionita[1], V. Naulin[2], J.J. Rasmussen[2], H.W. Müller[3], N. Vianello[4], Ch. Maszl[1], V. Rohde[3], M. Zuin[4], R. Cavazzana[4], M. Maraschek[3], ASDEX Upgrade Team[3]

[1]*Association EURATOM/ÖAW, Institute for Ion Physics and Applied Physics, University of Innsbruck, Austria*
[2]*Association EURATOM/RISØ-Technical University of Denmark, Roskilde, Denmark*
[3]*Max-Planck-Institut für Plasmaphysik, EURATOM Association, Garching, Germany*
[4]*Consorzio RFX, Associazione Euratom-ENEA sulla Fusione, Padova, Italy*

Abstract: A probe head, combining electrostatic and magnetic probes, was used on the midplane manipulator and inserted into the scrape-off layer (SOL) of ASDEX Upgrade (AUG). The electric signals of six probe pins allow the determination of turbulent radial particle flux, Reynolds stress and radial flux of poloidal momentum. Here special emphasis is laid on the momentum flux, revealing the fine structure of single ELM filaments. Magnetic signals were analyzed in order to recognize the occurrence of possible current filaments associated to type I ELMs. From the components of the magnetic field perturbations we obtain hodograms, which are direct indications of ELM current filaments aligned with the ambient magnetic. The results are compatible with the existence of toroidal current filaments as predicted by various ELM theories.

Probe head for simultaneous registration of electric and magnetic signals in the SOL of AUG:

Probe 1: floating, radially protruding by 3 mm, $V_{fl,1}$
Probe 2: floating, $V_{fl,2}$
Probe 3: floating, $V_{fl,3}$
Probe 4: negatively biased, $I_{is,4}$
Probe 5: swept, T_e
Probe 6: floating, $V_{fl,6}$

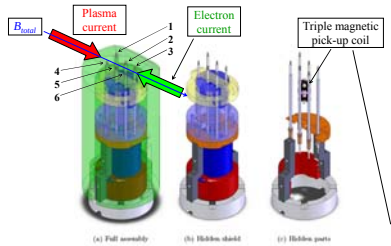

Front view of the probe head (as seen from the plasma):

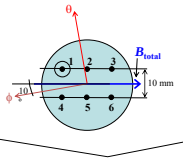

One magnetic triple sensor 20 mm behind the front side.

Triple magnetic sensor for measuring variations of b_r, b_ϕ and b_θ consisting of three coils of 0,2 mm diameter wire, wound around a small parallelepiped of Vespel of 7×7×8 mm³ dimensions.

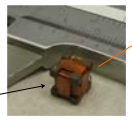

Probe head mounted on the midplane manipulator of AUG and inserted up to three times during an average AUG shot of 7 s length

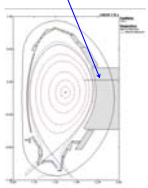

Penetration of the probe into the scrape-off layer (SOL)

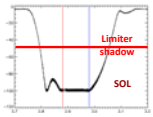

Radial position of the probe head with respect to the rest position.

Electric signals – radial transport of poloidal momentum during ELMs

This probe arrangement allows the determination of poloidal and radial electric field and plasma density ($d_{36} = 10$ mm in poloidal direction, $d_{12} = 3$ mm in radial direction):

$$E_\theta = \frac{V_{fl,6} - V_{fl,3}}{d_{36}} \qquad E_r = \frac{V_{fl,2} - V_{fl,1}}{d_{12}} \qquad n_{pl} \cong \frac{I_{is,4}}{eA_p}\sqrt{\frac{m_i}{k_B T_e}}$$

Of course, here we have to assume that the electron temperature is the same on all probe pin positions!! (It would be better to use emissive probes but this is not yet possible.)

From these results, the radial particle transport Γ_r, the Reynolds stress $\mathcal{R}_\theta$ and the radial transport of poloidal momentum M_r can be derived:

$$\Gamma_r = \tilde{n}\tilde{v}_r = \frac{\tilde{n}\tilde{E}_\theta}{B_\phi} \qquad \mathcal{R}_\theta = n_0\tilde{v}_r\tilde{v}_\theta = \frac{n_0\tilde{E}_\theta\tilde{E}_r}{B_\phi^2} \qquad M_r = \frac{nE_\theta E_r}{B_\phi^2}$$

With n and $v_{r,\theta}$ being defined as $X = X_0 + X_\theta$, the momentum flux splits up into four contributions:

$$M_r = \mathcal{R}_\theta + v_{0,\theta}\Gamma_r + n_0 v_{r,0} v_{\theta,0} + n_0 v_{r,0} v_{\theta,0}$$

The first term of M_r contains the Reynolds stress and the second one is the convective momentum flux containing the radial particle flux. The third term is composed of only fluctuating quantities. The fourth term of M_r does not contribute on average, because if the average is taken over the entire time, we see that $\langle n_0 v_{r,0} v_{\theta,0}\rangle = n_0 v_{\theta,0}\langle v_{r,0}\rangle = 0$.

Integrated radial flux of poloidal momentum during L-Mode and H-mode

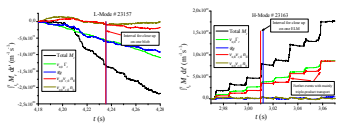

(a) (b)

Total momentum is shown as black line, the other lines show the parameters listed; (a) during L-mode discharge #23157, (b) during H-mode #23163; the red and blue vertical lines delimit the time interval of the single blob and ELM, respectively, shown in the figures on the right hand side.

The integrated flux of momentum shows a stepwise increase during the H-mode and a continuous decrease during the L-Mode. The steps in the H-mode correspond to ELMs. The fluxes in H-mode and L-mode have different signs on average. Here positive sign means outward transport of positive poloidal momentum.

Instantaneous and integrated radial flux of poloidal momentum during H-mode – close-ups

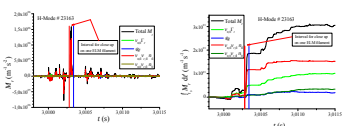

(a) (b)

Instantaneous (a) and integrated (b) momentum flux during the ELM time interval delimited by the red and blue vertical line in the previous figures; total momentum (black line), the other lines show the parameters listed. The red and blue vertical lines delimit the time interval of the single ELM filament shown in the figure (a) on the right hand side.

In the close-up of one ELM the filamentary structure is visible. In the very big event at $t \approx 3{,}0103$ s the nonlinear component ($v_{\theta,0}v_{r,0}n_0$ - red line) is nearly twice as big as the convective component ($v_{\theta,0}\Gamma_r$ – green line).

Radial flux of poloidal momentum during H-mode and L-Mode– further close-ups

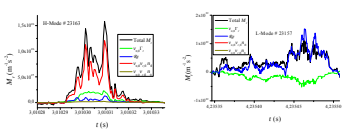

(a) (b)

Close up of the transport events shown in the previous figures by the red and blue lines. Total momentum (black line), the other lines show the parameters listed; (a) one filament during an ELM, (b) during blob events in the L-mode.

In the close-up on one ELM filament in H-mode and one blob event during L-mode the dominating components of the flux ($v_{\theta,0}\Gamma_r$ and $v_{\theta,0}v_{r,0}n_0$ for H-mode, $v_{\theta,0}\Gamma_r$ and $\mathcal{R}_\theta$ for L-Mode) are shown. The flux components do not always have the same sign.

Magnetic signals – ELM current filaments

Raw magnetic signals and hodograms

Discharge # 23159

(a) Temporal evolution of I_{sat} (black line).
(b) Temporal evolution of b_r (black line) and b_θ (blue line) Blue and orange bars show time intervals for the hodograms in (c).

A phase jump of π/2 occurs in the blue and orange intervals

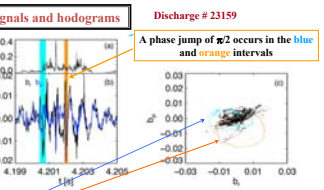

(c) Due to phase jumps in the blue and orange intervals in (b), we obtain closed loop hodograms (in corresponding colours), which are indications of current filaments aligned mainly in toroidal direction. The black curve shows the hodogram of the inter-ELM time intervals of (b), yielding a different pattern in between ELMs without closed loops.

Spectrogram of DOP

Discharge # 23159

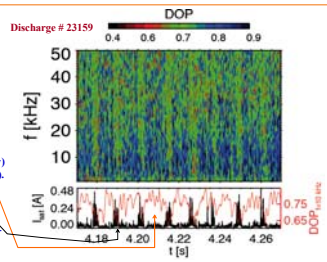

The Degree of Polarisation (DOP) analysis helps us to distinguish wave structures and localized coherent structures.

With reference to the I_{sat} signal, during inter-ELM intervals, DOP > 0,8 ⇒ plasma waves (MHD activity) (dark blue and black ranges).

During ELM intervals, DOP < 0,8 ⇒ strongly localized coherent structures interpreted as current carrying filaments (green and red ranges).

Three-dimensional hodogram

Discharge # 23159

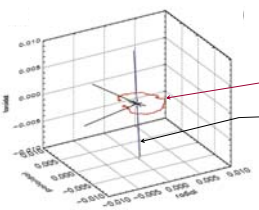

3-D trajectory of all 3 component of *B*-field fluctuations spans a well defined surface with a much smaller fluctuation in the parallel direction. The closed elliptical loop lies in a plane slightly tilted with respect to the local frame of reference.

The direction normal to the plane of the ellipse can be determined by using the minimum variance analysis (black line). This direction coincides well with the direction of B_{total} (blue line).

Two-dimensional reconstruction by the maximum variance analysis

A 2-D reconstruction in the reconstructed maximum variance plane shows that the magnetic fluctuations are generated by a *monopolar* current distribution (red line = elliptical fit, discharge #23159). This is also supported by the fact that the loop lies practically only in two quadrants of the plane. A bipolar loop would span over three quadrants.

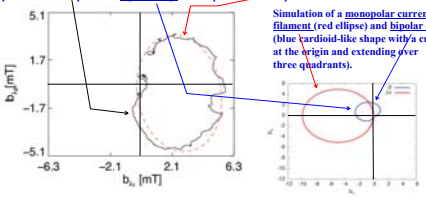

Simulation of a monopolar current filament (red ellipse) and bipolar one (blue cardioid-like shape with a cusp at the origin and extending over three quadrants).

Monopolar or bipolar current filament?

An ELM is a density filament produced by a peeling-ballooning perturbation in the SOL.

If currents are associated to these density filaments, their projection in the perpendicular plane should look like that:
(a) in case of a monopolar current filament,
(b) in case of a bipolar current filament

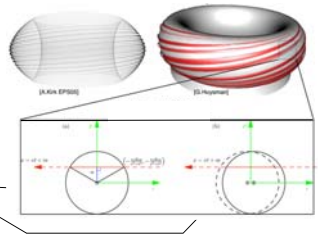

Determination of current, current density and distance from probe

Schematic of a monopolar filament moving towards the probe with an assumed velocity $v_x = 1$ km/s mainly in radial direction *x* but in reality with also a poloidal component; *x*, *y* are two coordinates perpendicular to each other in the plane perpendicular to the filament axis.

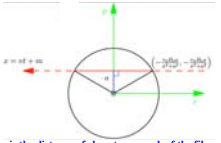

a is the distance of closest approach of the filament to the probe, which can be estimated for constant v_x: $a = \Delta t\, v_x$

Δt is the time delay between the maximum of b_x and the maximum/minimum of b_y.

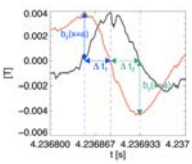

These are indeed the expected signals for the two components of *b* during such an event.

Conclusion: Assuming a monopolar filament flowing with velocity v_x, the current can be estimated noting that:

$$b_x = -\frac{r_0 B_0 a}{x^2 + a^2} \quad \text{and} \quad b_y = \frac{r_0 B_0 x}{x^2 + a^2} \quad \text{with} \quad B_0 = \frac{\mu_0 I_0}{2\pi r_0}$$

Consequently

$$b_y(x = a) = \frac{\mu_0 I_0}{4\pi a} \Rightarrow b_y(x = a) = \frac{\mu_0 I_0}{4\pi v_x \Delta t}$$

Based on these assumptions we obtain a current I_0 = 1,7 kA. With 1 cm radius of the filament this corresponds to a current density up to 6 MA/m².

C. Ioniță, N. Vianello, H.W. Müller, F. Mehlmann, M. Zuin, V. Naulin, J.J. Rasmussen, V. Rohde, R. Cavazzana, C. Lupu, M. Maraschek, R.W. Schrittwieser, P.C. Balan, ASDEX Upgrade Team, "Simultaneous measurements of electrostatic and magnetic fluctuations in ASDEX Upgrade edge plasma", *Journal of Plasma and Fusion Research Series* **8** (2009), 413-418.
E. Martines, N. Vianello, D. Sundkvist, M. Spolaore, M. Zuin, M. Agostini, V. Antoni, R. Cavazzana, C. Ionita, M. Maraschek, F. Mehlmann, H.W. Müller, V. Naulin, J.J. Rasmussen, V. Rohde, P. Scarin, R. Schrittwieser, G. Serianni, E. Spada, RFX-mod team, ASDEX Upgrade team, "Current filaments in turbulent magnetized plasmas", *Plasma Physics and Controlled Fusion* **51** (2009), 124503 (11pp) (doi: 10.1088/0741-3335/51/12/124053).
R.W. Schrittwieser, C. Ionita, N. Vianello, H.W. Müller, F. Mehlmann, M. Zuin, V. Naulin, J.J. Rasmussen, V. Rohde, R. Cavazzana, C. Lupu, M. Maraschek, C. Maszl, ASDEX Upgrade Team, "A probe head for simultaneous measurements of electrostatic and magnetic fluctuations in ASDEX Upgrade edge plasma", *Contributions to Plasma Physics*, in print.
N. Vianello, V. Naulin, R. Schrittwieser, H.W. Müller, M. Zuin, C. Ionita, J.J. Rasmussen, F. Mehlmann, V. Rhode, R. Cavazzana, M. Maraschek, C. Lupu, ASDEX Upgrade team, "Direct observation of current in ELM filaments on Asdex Upgrade", *arXiv:0910.2362, Physical Review Letters*, submitted.
V. Naulin, N.Vianello, R. Schrittwieser, H.W. Müller, P. Migliucci, M. Zuin, C. Ionita, Ch. Maszl, F. Mehlmann, J.J. Rasmussen, V. Rohde, R. Cavazzana, M. Maraschek, the ASDEX Upgrade team, and JET EFDA contributors, "Magnetic diagnostic of SOL-filaments generated by type I ELMs on JET and ASDEX Upgrade", *Journal of Nuclear Materials*, submitted;

Acknowledgements: This work, supported by the European Communities under the Contracts of Associations between EURATOM and ÖAW, IPP, ENEA-RFX and RISØ, was carried out within the framework of the EFDA. The content of the publication is the sole responsibility of its authors and it does not necessarily represent the views of the Commission or its services. This work was also supported by grant P19901 of the Austrian Science Fund (FWF).